Journal of Computation and Artificial Intelligence in Mechanics and Biomechanics ISSN 2184-8971
Volume 1, Issue 2, Page 36-41, 2021

Estimating active forearm pronation-supination motion by means of FE modelling

Sánchez-Arce, I. J.[1]

[1] *Instituto de Ciência e Innovação em Engenharia Mecânica e Engenharia Industrial (INEGI); Rua Dr Roberto Frias 400, Campus da FEUP;4200-465; Porto;Portugal*

Abstract
Active range of motion (ROM) of the forearm is important for completing daily life activities (ADL). Such motion could be compromised as a result of a poorly healed fracture. Although numerical models are often used to aide medical treatment, most of them are static. In addition, there is no previous model nor methodology related to forearm and its motion. In this work, a methodology to create finite element models that can evaluate active ROM is developed and validated. The biomechanical behaviour of the ligamentous structures, as a whole, was compared with data available from previous studies. The active ROM was validated against experimental measurements of active ROM. The ROM predicted with this methodology was 72º in pronation and 83º in supination; these values are within 5º from the standardised values for human ROM. In addition, this work supports the hypothesis that the muscles are limiting structures of the ROM, such task was always attributed to ligamentous structures. Nevertheless, in active ROM, muscle contraction and extension delimited the arc of motion. In summary, this work provides a methodology, mechanical properties of ligamentous structures, types of constrains and kinematic assumptions to produce a biomechanically sound model of the forearm which can be used for further study of forearm fractures.

***DOI**: 10.5281/zenodo.4837374*

Article Info

Keywords
Finite element method
Human forearm models
Pronation-supination motion
Connector elements
Active forearm motion

Article History
Received: 29/10/2020
Revised: 01/02/2021
Accepted: 26/03/2021

1 Introduction

Forearm rotational motion is necessary for performing daily life activities (ADL) [1], [2]. It is known that malunion of forearm fractures can produce changes in forearm rotational range of motion (ROM), commonly reducing it [3]–[5]. The distal radius fracture (DRF) is the most common frequent. It has also been hypothesised that malunited DRFs could produce changes in the force transmitted in the distal radioulnar joint (DRUJ) [6].

Finite element modelling (FEM) has been used to analyse: a) the force transmitted at the DRUJ [7], and b) the effects of malunited forearm fractures [8]–[10]. However, no evidence of previous models that consider the bone motion or static models of the whole forearm has been found in the literature. Therefore, a complete methodology which takes into account the soft tissue structures involved in the pronation-supination (P-S) motion and their mechanical properties has to be developed. Also, models of the full forearm are necessary for this, which are also rare in the literature.

This paper aims to establish a methodology to develop FE models of the forearm that allow estimating P-S motion. Therefore, bone geometries form two forearms were extracted from computed tomography (CT) scans. Soft tissues involved in the P-S motion were identified and their mechanical properties were obtained from the literature. Once the proposed methodology is validated, it can be applied to modelling bones with malunited fractures for further studies, for example, changes in the ROM.

2 Methodology

2.1. Bone and cartilage geometries

Forearm geometry was extracted from computed tomography (CT) scans provided by the Wrightington Hospital. Image size was 512 x 512 pixels, the slice size was 500 μm. The left forearm corresponds to a 27-year-old male, the right to a 37-year-old female. The CT scans were segmented using ScanIP software (ScanIP 3.2, Simpleware LTD) following the procedure described in [11], [12]. Both cortical and trabecular bone layers were segmented separately, resulting in a more accurate bone representation. The bone geometry was exported as 'point cloud'; later, it was converted to solid geometry using SolidWorks (SolidWorks 2012, Dassault Systèmes). Finally, the solid models were imported into Abaqus (Abaqus 6.12, Dassault Systèmes).

Corresponding Author:
I.J. Sánchez-Arce
isidrodjsa@gmail.com

Cartilages were created in ScanIP by expanding the cortical bone surfaces. Cartilage thickness was considered constant and was determined as half of the minimum distance between articular surfaces. Afterwards, cartilage profiles were trimmed following anatomic descriptions, i.e., [13]. The cartilages correspond to the DRUJ and the proximal radioulnar joint (PRUJ). Finally, cortical and trabecular bone layers, as well as cartilages, were joint in Abaqus through Boolean operations.

2.2. Ligamentous structures and muscles

Two ligamentous structures stabilise the forearm motion, the distal radioulnar ligaments (DRUL) and the interosseous membrane (IOM). The DRUL connect the distal portions of the ulna and radius. The IOM connects the radius to the ulna along their shafts. The DRUL stabilises the pronation-supination motion. Although the IOM also stabilises the motion, its main function is to transmit load from the radius to the ulna. The IOM is composed of five regions, from which locations related to bone length can be calculated following the suggestions and proportions given by Noda et. al., [14]. A 'reference point'(RP) was positioned at the corresponding location; later, each RP was attached to a surface area, as anatomically as possible, through a 'kinematic coupling'; this process allowed to reduce stress concentration in attachment points. Afterwards, a spring element was placed between the anatomical locations, as shown in Figure 1a. All the springs were considered as tension-only and their stiffness was calculated as a function of their anatomical cross-sectional areas, which were reported by [14]–[16]; for the 'Distal accessory band' no area was found; however, in a later study Werner reported its stiffness [16]. The data was validated using areas and stiffness values from [14], [15]. The stiffness of each region is reported in Table **1**. Similarly, for the DRUL, their stiffness was calculated from the work of Schuind et. al., [17]; however, unlike them, in this work, both upper and lower DRUL regions were considered, as shown in Figure 1c. The DRUL mechanical stiffness values are listed in Table 2.

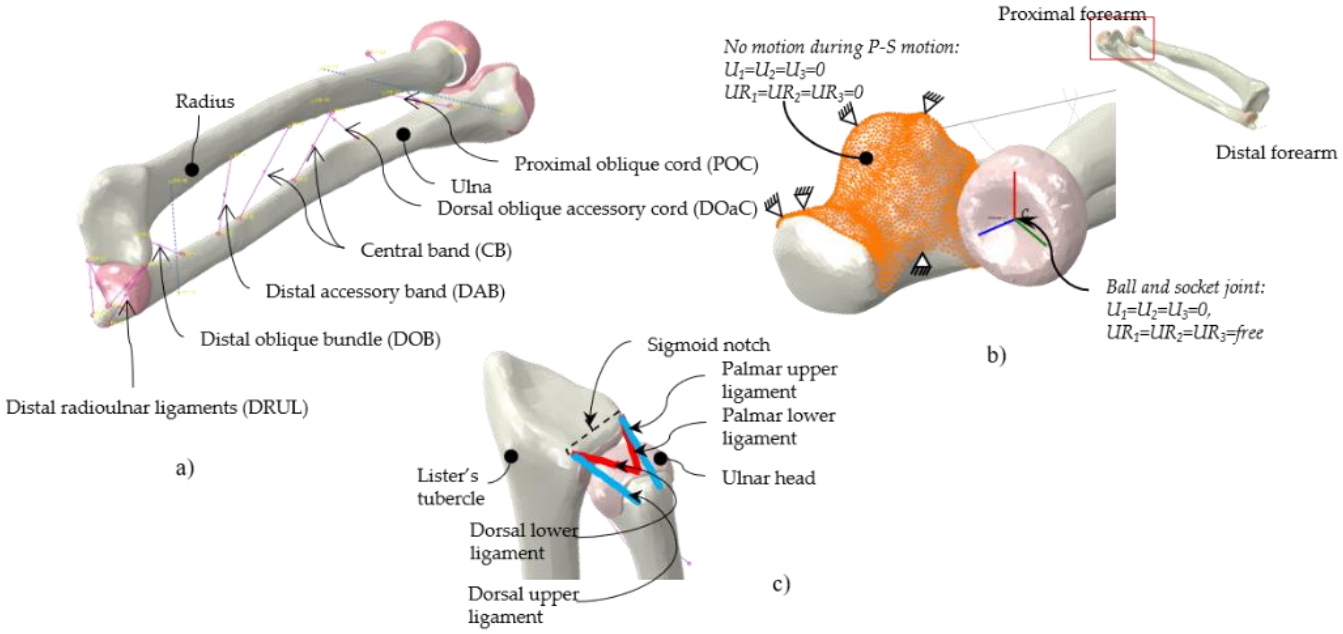

Figure 1. Interosseous membrane locations a), boundary conditions at the ulnar trochlea and radial head b), and the distal radioulnar ligaments c).

Table 1. Cross-sectional areas [14], and calculated individual stiffness for each IOM region.

IOM region	Cross-section area *(mm²)*	Stiffness *(N/mm)*
Central band (CB) (2 bundles)	12.61	103.24
Distal accessory band (DAB) [16]	--	11.2
Dorsal oblique bundle (DOB)	6.6	54.04
Proximal oblique cord (POC)	4.07	33.32
Dorsal oblique accessory cord (DOaC)	2.88	23.58

Subsequently, the biomechanical behaviour of the assembly was verified by numerically reproducing the experimental work performed by Hotchkiss et. al., [18], a good agreement was found. Although, the PRUJ anatomically possesses a complex arrangement of ligaments it also behaves kinematically as a ball and socket joint [7]. Consequently, this behaviour was represented by placing a connector element (CONN3D2) at the centre of the

radial head, and kinematically coupled to it. The connector element was configured to behave as a ball and socket joint (Figure 1b). Finally, the ulnar trochlea was fixed, as shown in Figure 1b.

On the other hand, it has been hypothesised that muscles cannot extend or contract beyond their anatomical limits, and so they can behave as a mechanical stop [19], [20]. Consequently, these structures could be used to determine the theoretical range of motion after a malunited fracture is present. Similarly, as it was done with the IOM and DRUL, the attachment points for the prime forearm movers were created and kinematically coupled to the bone surfaces (Figure 2) following the anatomical locations described by [13], [21], [22]. The prime movers are the pronator quadratus (PQ), pronator teres (PT), and the supinator muscle (Sup). These muscles were also simulated with a connector element configured as a tension-only spring in parallel to a contractile element, like Hill's muscle model. Therefore, active pronation-supination was achieved. The spring part of each connector was used as antagonist element. The antagonist force was determined from the measured change on length of each connector element and the electromyographic force reported by Gonzalez et. al., [23] during the pronation-supination motion. The resulting stiffness for each connector were: PQ=19.3 N/mm, PT=35.1 N/mm, and Sup=8.4 N/mm. Finally, the length of each connector representing a muscle was recorded, which will be used for further study of ROM reduction.

Table 2. Stiffness of each DRUL, values based on [17].

Ligament	Stiffness (*N/mm*)
Upper dorsal	6.6
Lower dorsal	6.6
Upper palmar	5.5
Lower palmar	5.5

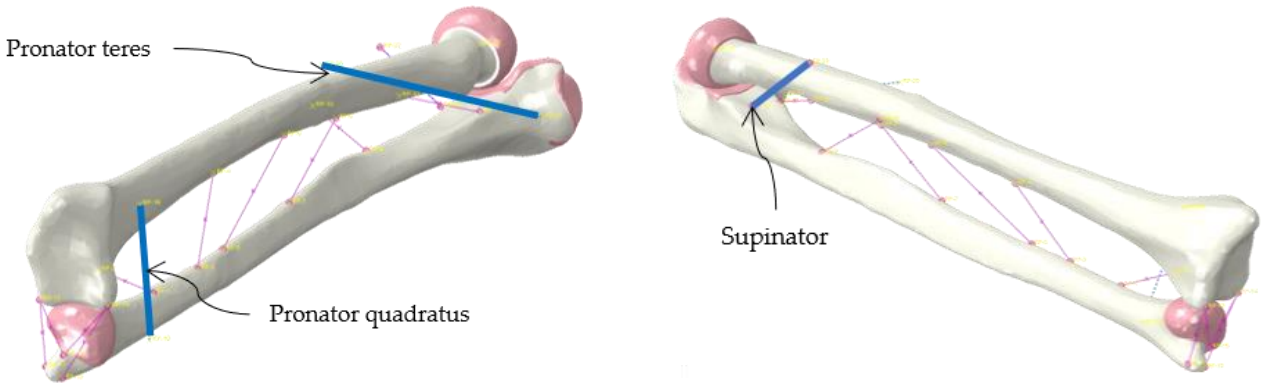

Figure 2. Forearm's prime movers simulated as connector elements.

ROM achieved was calculated from the initial and final coordinates of a few bony landmarks: ulnar and radial styloid processes, and the midpoint of the sigmoid notch, as shown in Figure 3. Once the simulation was completed, the coordinates of each point, throughout the full simulation, were exported as a spreadsheet (XSLX file).

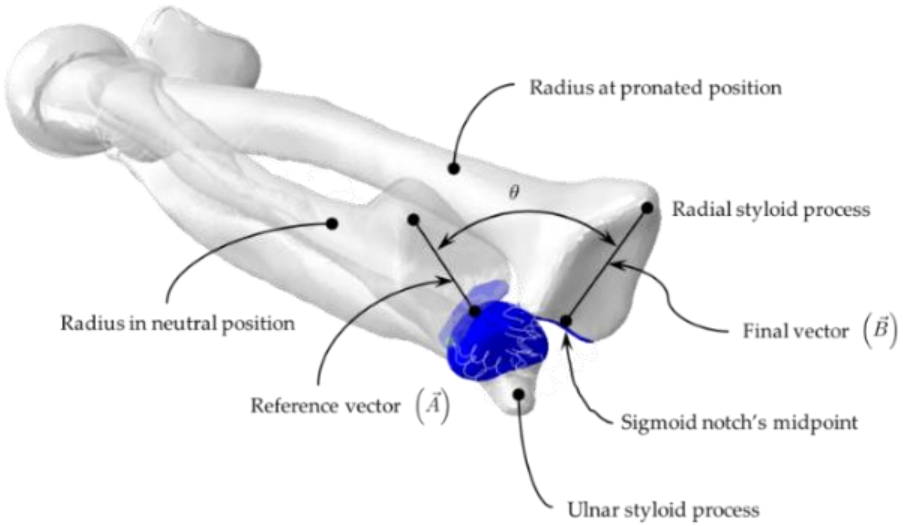

Figure 3 Anatomic bony landmarks for determining the model's ROM.

The ROM was calculated by means of the dot product between $\vec{A}$ and $\vec{B}$ (Figure 3). The angle was then calculated.

2.3. Mechanical properties, meshing and loading

Bone and cartilage were considered as linear-elastic materials because, at this stage, the models are focused on estimating ROM. The mechanical properties of bone and cartilage were taken from previous modelling of the wrist [8], [24], and are listed in Table 3.

Table 3. Mechanical properties of bone layers and cartilage used in the FE models.

Layer	Young's modulus (*MPa*)	Poisson's ratio
Cortical bone [24]	18000	0.20
Trabecular bone [24]	100	0.25
Cartilage [8]	10	0.30

The models were meshed using four-node tetrahedral elements (Abaqus C3D4). Element size varied according to the geometric regions of each bone. Element size was minimum in cartilaginous areas, muscle and ligament attachment regions, and areas where the cortical bone was thin, e.g., sigmoid notch area and ulnar trochlea. The number of nodes and elements were 112519 and 550255, respectively for the left model. The right model had 110056 nodes and 557555 elements.

Active motion was achieved by applying a negative displacement (contraction) to the connector elements representing the PQ and the Sup. Pronation was produced by applying -15.5 mm to the left PQ and -11.4 mm to the right PQ. Similarly, supination was produced by a -16.2 mm in the left model and -12.0 mm to the right model. The displacement applied to each connector was determined from previous testing of the model, as it was done for their antagonistic forces; in this case, to the range prior dislocation of the DRUJ. This had to be performed because the muscle length depends on the person's morphology; moreover, little information is available regarding these lengths, and so when morphologic specific data is required, it has to be extracted from medical images. However, no more data was available from the subjects who provided the CT scans.

3 Results

3.1. Range of motion

The left forearm model achieved a ROM of 71.4° and 82.4° for pronation and supination, respectively. The right forearm model reached 73.2° and 83.5°, respectively. These values are reported in Figure 4. These values were also compared with the 'anatomical' ROM described by the American Academy of Orthopaedic Surgeons (AAOS) [25] and with experimental measurements of active ROM from a control group (CG) composed of healthy individuals [26]. A difference of less than 3% was found (range 0.5% to 3%) with the data reported by the AAOS. On the other hand, a difference of less than 5% (range 3% to 4.4%) with the experimental data was observed.

3.2. Muscle lengths

As the models reached an active ROM consistent to anatomical measurements; in addition, it has been hypothesised that the muscle length also act as a limiting factor to the ROM [19], [20]. Consequently, the maximum and minimum length of each simulated muscle was recorded and reported in Table 4. Thus, these lengths would be used as constrains within the connector element configuration for further studies using these FEM and their variants.

Table 4. Maximum and minimum lengths of the simulated muscles.

	Length (mm)			
	Left		Right	
Muscle	Maximum	Minimum	Maximum	Minimum
Pronator quadratus	45.3	24.0	37.8	25.3
Pronator teres	102.5	87.8	96.4	85.6
Supinator	37.6	16.8	30.8	20.5

4 Discussion and conclusion

The main objective of these models was to simulate ROM; nevertheless, the geometry was created as accurate as possible, which increase the capability of the models for future analyses of stress and strain distributions in the bone surface. In this work, the IOM was represented with springs, one spring for each IOM region. Although stiffness of each region was theoretically calculated from a series of cadaveric studies, the agreement of the full assembly with another cadaveric study indicates that the proposed representation and stiffness of the IOM is anatomically representative.

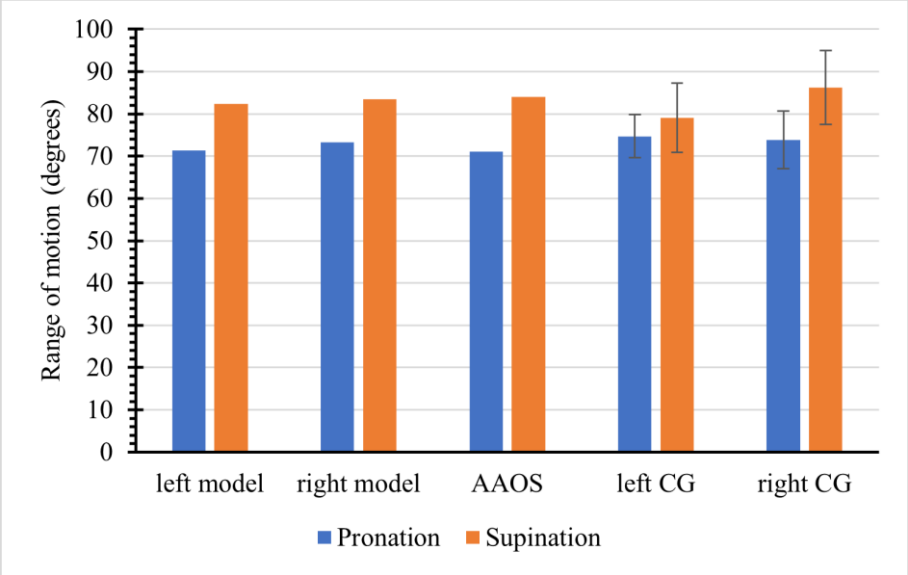

Figure 4. Comparison between the ROM obtained from the FEM models, and those from the American Academy of Orthopaedic Surgeons (AAOS), and from a Control Group (CG) texted experimentally by the author [26].

The assumption of considering the PRUJ as a ball and socket joint agreed with the kinematic models of forearm motion [27]. The chosen boundary conditions represent this ball and socket behaviour. This behaviour has been recently represented in other FE studies [23,24], in which the boundary conditions corresponding to the radial head are equal to those proposed here; however, those models did not investigate the forearm ROM. The motion was produced by the contraction of linear elements (connectors) and no motion axes were defined; thus, the radius rotates freely upon the ulnar surface. This is an advantage because geometrical changes are a consequence of a distal radius malunion, which also changes the position of the muscle attachment points. A similar concept was found in the literature, they were using springs to produce the motion [28], but antagonistic effects were not considered, whilst in this project both agonist and antagonist effects of the muscles were considered.

The achieved ROMs are close to the 'normal' ROM suggested by the AAOS [25]. The variation between the recommended and the achieved ROM is less than 10°, which according to clinical practice can be considered as a good agreement [29]. Similarly, the achieved ROM from the models are within the limits of an in-vivo study performed in healthy volunteers [26], with a difference of less than 5°. It was decided to use the recommended ROM because of the anatomic differences between the models; moreover, motion and morphology differences also exist amongst the volunteers conforming the experimental studies (e.g., CG and literature). In consequence, using a 'normal ROM' allow the results extracted from these models to be in a similar range to those available from other sources.

The use of connector elements for simulating the forearm active muscles provided a good alternative to simulate active forearm motion; moreover, the length of these elements (Table 4) provided to be a method for limiting the ROM in the models. This complies with the hypothesis of the muscles as limiting factors proposed by [19], [20]. Although that the muscle length has been anatomically considered as a limiting factor to the ROM, no evidence of its use in previous modelling work has been found. This approach, however, does not consider the wrapping of the muscle over the bone surfaces, which applies the force tangent to the surface. The use of banded ligamentous structures created from 'magnetic resonance images' (MRI) has been proposed by Gislason [12]; however, it was applied to a static model; in addition, it would require even more computational power because of the number of elements and the amount of contact interactions required. In addition, to the author's knowledge this is the first numerical model evaluating active forearm motion. Moreover, this work has also proved that the muscles had an effect in limiting the forearm motion, such effect was often attributed to ligamentous structures.

In conclusion, the methodology briefly described in this work can produce biomechanically sound FE models that can be used for studying limb rotational motion, like the forearm pronation-supination. Moreover, the calculated stiffness values for each of the regions of the interosseous membrane is a secondary contribution that could benefit FE models, like those used to analyse load distribution for radial head prostheses.

Acknowledgements and Funding

The author thanks CONACyT (Consejo Nacional de Ciencia y Tecnología) Mexico for the scholarship that made possible this research. Moreover, thanks Prof Teresa Alonso and Dr Alan Walmsley for their advice during the development of this work. Finally, thanks to Prof Adam C Watts for the CT scans necessary to create the 3D models.

References

[1] B. F. Morrey, L. J. Askew, and E. Y. S. Chao, "A biomechanical study of normal functional elbow motion.," *J. Bone Joint Surg. Am.*, vol. 63, no. 6, pp. 872–7, Jul. 1981.
[2] M. Sardelli, R. Z. Tashjian, and B. A. MacWilliams, "Functional Elbow Range of Motion for Contemporary Tasks," *J. Bone Jt. Surg.*, vol. 93, no. 5, pp. 471–477, 2011.
[3] G. S. Fraser, L. M. Ferreira, J. A. Johnson, and G. J. W. King, "The Effect of Multiplanar Distal Radius Fractures on Forearm Rotation: In Vitro Biomechanical Study," *J. Hand Surg. Am.*, vol. 34, no. 5, pp. 838–848, 2009.
[4] H. Hirahara, P. G. Neale, Y.-T. Lin, W. P. Cooney, and K.-N. An, "Kinematic and torque-related effects of dorsally angulated distal radius fractures and the distal radial ulnar joint," *J. Hand Surg. Am.*, vol. 28, no. 4, pp. 614–621, 2003.
[5] L. M. Ferreira, G. S. Greeley, J. A. Johnson, and G. J. W. King, "Load transfer at the distal ulna following simulated distal radius fracture malalignment.," *J. Hand Surg. Am.*, vol. 40, no. 2, pp. 217–23, Feb. 2015.
[6] B. D. Adams, "Effects of radial deformity on distal radioulnar joint mechanics," *J. Hand Surg. Am.*, vol. 18, no. 3, pp. 492–498, 1993.
[7] D. Greybe, M. R. Boland, T. Wu, and K. Mithraratne, "A finite element model to investigate the effect of ulnar variance on distal radioulnar joint mechanics.," *Int. j. numer. method. biomed. eng.*, Mar. 2016.
[8] D. D. Anderson, B. R. Deshpande, T. E. Daniel, and M. E. Baratz, "A three-dimensional finite element model of the radiocarpal joint," *Iowa Orthop. J.*, vol. 25, p. 10, 2005.
[9] J. Tan, M. Mu, G. Liao, Y. Zhao, and J. Li, "Biomechanical analysis of the annular ligament in Monteggia fractures using finite element models," *J. Orthop. Surg. Res.*, vol. 10, no. 1, p. 30, 2015.
[10] T. Miyake, H. Hashizume, H. Inoue, Q. Shi, and N. Nagayama, "Malunited Colles' fracture Analysis of stress distribution," *J. Hand Surg. Br. Eur. Vol.*, vol. 19, no. 6, pp. 737–742, 1994.
[11] Simpleware_LTD, "ScanIP, ScanFE and ScanCAD version 3.1; Tutorial guide." Simpleware LTD, 2008.
[12] M. K. Gíslason and D. H. Nash, "Finite element modelling of a multi-bone joint: the human wrist," in *Finite Element Analysis - New Trends and Developments*, F. Ebrahimi, Ed. InTech, 2012.
[13] N. Palastanga, R. Soames, and D. Field, *Anatomy and human movement: structure and function*, 4th ed. Edinburgh: Butterworth-Heinemann, 2002.
[14] K. Noda, A. Goto, T. Murase, K. Sugamoto, H. Yoshikawa, and H. Moritomo, "Interosseous Membrane of the Forearm: An Anatomical Study of Ligament Attachment Locations," *J. Hand Surg. Am.*, vol. 34, no. 3, pp. 415–422, 2009.
[15] H. J. Pfaeffle *et al.*, "Tensile properties of the interosseous membrane of the human forearm," *J. Orthop. Res.*, vol. 14, no. 5, pp. 842–845, 1996.
[16] F. W. Werner, J. L. Taormina, L. G. Sutton, and B. J. Harley, "Structural properties of 6 forearm ligaments.," *J. Hand Surg. Am.*, vol. 36, no. 12, pp. 1981–7, Dec. 2011.
[17] F. Schuind *et al.*, "The distal radioulnar ligaments: A biomechanical study," *J. Hand Surg. Am.*, vol. 16, no. 6, pp. 1106–1114, 1991.
[18] R. N. Hotchkiss, K.-N. An, D. T. Sowa, S. Basta, and A. J. Weiland, "An anatomic and mechanical study of the interosseous membrane of the forearm: Pathomechanics of proximal migration of the radius," *J. Hand Surg. Am.*, vol. 14, no. 2, Part 1, pp. 256–261, 1989.
[19] M. S. Feeney, F. Wentorf, and M. D. Putnam, "Simulation of altered excursion of the pronator quadratus.," *J. Wrist Surg.*, vol. 3, no. 3, pp. 198–202, Aug. 2014.
[20] C. C. Norkin and D. J. White, *Measurement of joint motion: a guide to goniometry*, Fifth. F. A. Davis Company, 2016.
[21] C. Fontaine, F. Millot, D. Blancke, and H. Mestdagh, "Anatomic basis of pronator quadratus flap," *Surg. Radiol. Anat.*, vol. 14, no. 4, pp. 295–299, 1992.
[22] H. Gray, *Gray's Anatomy*, 35th editi. London: Longman Group LTD, 1973.
[23] R. V Gonzalez, E. L. Hutchins, R. E. Barr, and L. D. Abraham, "Development and evaluation of a musculoskeletal model of the elbow joint complex," *J. Biomech. Eng.*, vol. 118, no. 1, pp. 32–40, 1996.
[24] M. K. Gíslason, B. Stansfield, and D. H. Nash, "Finite element model creation and stability considerations of complex biological articulation: The human wrist joint," *Med. Eng. Phys.*, vol. 32, no. 5, pp. 523–531, 2010.
[25] D. C. Boone and S. P. Azen, "Normal range of motion of joints in male subjects.," *J. Bone Joint Surg. Am.*, vol. 61, no. 5, pp. 756–9, Jul. 1979.
[26] I. de J. Sánchez-Arce, A. Walmsley, M. Fahad, and E. S. Durazo-Romero, "Lateral differences of the forearm range of motion," *J. Eng. Med.*, vol. 234, no. 5, pp. 496–506, 2020.
[27] A. M. Weinberg, I. T. Pietsch, M. B. Helm, J. Hesselbach, and H. Tscherne, "A new kinematic model of pro- and supination of the human forearm," *J. Biomech.*, vol. 33, no. 4, pp. 487–491, 2000.
[28] S. Shimawaki, M. Ebe, M. Nakabayashi, and N. Sakai, "Simulation of the stabilizing mechanism of distal radioulnar joint during pronation and supination," *J. Biomed. Sci. Eng.*, vol. 8, no. 3, p. 15, 2013.
[29] A. D. Armstrong, J. C. MacDermid, S. Chinchalkar, R. S. Stevens, and G. J. W. King, "Reliability of range-of-motion measurement in the elbow and forearm.," *J. shoulder Elb. Surg.*, vol. 7, no. 6, pp. 573–580, 1998.